Heat transfer and flow performance of Impingement and Impingement/Effusion Cooling Systems

Dr. Assim H. Yousif,
Mechanical Engineering Department , University of Technology/Baghdad.
Assim_yousif20000@yahoo.com
Dr. Amer M. Al Dabagh
Mechanical Engineering Department , University of Technology/Baghdad.
aamermajeed@yahoo.com
Salah H. Abid Aun
Institute of Technology, Baghdad

Received on: 28/1/2015 & Accepted on:7/5/2015

Abstract:

The current experimental study is made to investigate the heat transfer characteristics and pressure losses for both impingement and impingement/effusion cooling systems. The experiments are carried out on a metal test plate. The numerical work is made to analyze the flow behavior in the test section. The benefit of introducing the present experimental method is the capability of investigating and analyzing the performance of both impingement and impingement/effusion cooling systems by the same test rig. The impinging jet device configurations are designed as inline round multi-hole arrays with jet to jet spacing of 4 jet hole diameter. The effusion holes configurations are inline round multi-hole arrays. Staggered arrangement between jet and effusion holes is maintained. The Jet Reynolds numbers (Re_j) of 5000 to 15000 and jet height to diameter ratio (H/D) of 1.5, 2.0, and 3.0 are maintained. For impingement/effusion case, the best wall cooling effectiveness is obtained at ($H/D = 2$), and maximum increment in the wall cooling effectiveness over that of impingement case is 23% at (Re_j= 5000), 16 % at (Re_j= 7500), and 14% at (Re_j= 15000). Jet spacing in impingement case and blowing ratio in impingement/effusion case show an evident effect on the discharge coefficients.

Keywords: Impingement, Impingement effusion, Cooling effectiveness, Discharge coefficient.

اداء انتقال الحرارة والجريان لأنظمة التبريد التصادمية والتصادمية/التغلغلية

الخلاصة:

https://doi.org/10.30684/etj.33.6A.20
2412-0758/University of Technology-Iraq, Baghdad, Iraq
This is an open access article under the CC BY 4.0 license http://creativecommons.org/licenses/by/4.0

الدراسة الاختبارية الحالية تبحث عن تحديد الخصائص الحرارية وخسائر الضغط لمنظومتي التبريد التصادمية والتصادمية/التغلغلية. الجانب النظري يشمل دراسة سلوك الجريان عند مقطع الاختبار. تم اجراء التجارب على صفيحة اختبار معدنية. ان الفائدة من تقديم المنهج العملي الحالي هو القدرة على اختبار وتحليل اداء منظومتي التبريد التصادمية والتصادمية/التغلغلية في منصة اختبار واحدة. تم ترتيب كل من ثقوب النفث وثقوب التغلغل خطيا مع اخذ المسافة بين مركزي فتحتي نفثين متجاورتين مساوية الى اربعة أضعاف قطر الفتحة وتم الحفاظ على ترتيب متعرج عند تداخل ثقوب النفث والتغلغل في مقطع الفحص. اجريت الاختبارات عند أرقام رينولدز النفاث التي تتراوح بين 5000 الى 15000 وبنسبة مسافة فتحة النفث عن الهدف الى قطرالفتحة (H/D) هو 1.5, 2, 3. لحالة النظام التصادمي/التغلغلي, تم الحصول على افضل فعالية لتبريد الجدار عند (H/D=2) وان نسبة التحسن في فعالية التبريد بالمقارنة مع النظام التصادمي هي 23% عند (Re_j= 5000) , 16%عند (Re_j= 7500) و 14%عند =(Re_j 15000). كما اظهرت المسافة بين فتحة النفث و سطح الهدف في النظام التصادمي ونسبة النفخ للنظام التصادمي/التغلغلي تأثيرات واضحة على معاملات ضياعات التصريف.

Nomenclature

A= Target plate surface area, m^2
A_h= Hole cross-sectional area, m^2
BR= Effusion blowing ratio = $\frac{\rho_s U_s}{\rho_\infty U_\infty}$.
C_D=Discharge coefficient.
D = Jet hole diameter, m
H = Jet to target spacing, m
L = Length of jet hole, m
$\dot{m}$ = Mass flow rate, kg/s
P= Jet to jet pitching, m
Re = Reynolds number
S= Jet to jet spacing, m
t= Thickness of the target plate, m
T= Temperature, degree centigrade
Tw = Wall temperature, degree centigrade
U = Velocity of flow, m/s
X = Local length of the plate for both target plate and effusion plates, m
Z = Local width of the plate for both target plate and effusion plates, m
η = Wall cooling effectiveness
$\overline{\eta}$ = Average wall cooling effectiveness
$\eta_{sa.}$= Spanwise average wall cooling effectiveness
ΔP = Change in pressure, N/m^2
ρ = Density of the air, kg/m^3

Subscript

av. = average
h = hole
in = inner target surface
j= jet
o, out = outer target surface
s = secondary flow
∞ = mainstream flow

INTRODUCTION

Over the last thirty years, there have been significant technological advances towards the reduction of temperature of the surface material that is in contact with hot gases, and one of these solutions is the use impingement cooling or impingement/effusion techniques. The combustor liner is typically protected by a combined jet and effusion cooling. To meet the demand of high turbine inlet temperature and to avoid the combustor liner materials from melting, it is strongly needed to develop and find an optimum cooling system to overcome this problem. For impingement cooling system, many efforts have been made in this field to get optimum design. The heat rate is strongly influenced by the geometry of the impinging jet device. In the relevant past studies, the researchers have examined different parameters that affects the impingement cooling system, for example, jet impingement angle, jet to jet spacing, jet Reynolds number, jet height to diameter ratio, and jet shape.

The ratio of spacing (H) between the target plate and jet exit and the jet diameter (D), arrangement and spacing between holes plays a major role in the impingement/effusion cooling systems. Avery few studies are made on the effect of H/D on the combined jet impingement with effusion. Several researchers in the past analyzed the impingement heat transfer for single and multiple jets with and without effusion film holes and ascertained its influence on flat surface of Perspex or low conductive material.

Al-Dabagh et al. [1] investigated experimentally and numerically the influence of impingement jet number on the pressure loss and heat transfer coefficient. Thermocouples were used to investigate temperature gradient and concluded that the effusion wall gives an additive heat transfer to the impingement jet. Hyung and Dong [2] studied experimentally the local heat/mass transfer characteristics for flow through effused perforated plates. Naphthalene sublimation was employed to determine the local heat/mass transfer coefficients on the effusion plate. The results showed that the high transfer region is formed at stagnation region. Yong et al. [3] experimentally investigated the effect of rib arrangements on an impingement/effusion cooling system. The naphthalene coated test plate was installed on the effusion plate for local mass transfer measurements. They found that the overall heat transfer is promoted when ribs are installed on the effusion surface. Sang et al. [4] investigated experimentally the cooling effectiveness of full–coverage film cooled wall of jets holes inclined at 35° and 90° with impingement jets. Infrared camera was used to measure the temperature of the cooled surface. It was shown that the 35° reveals a higher film cooling effectiveness than 90°. Zhang et al. [5] studied numerically three dimensional simulations of flow and heat transfer characteristics of impingement/effusion cooling, effect of center–to-center spacing of the effusion hole and blowing ratio on the cooling effectiveness. The authors found that the wall cooling effectiveness increases as the center spacing of adjusting holes decrease. Yang et al. [6] tested a new design series of pieces with different geometrical configuration and geometry dimensions to investigate the impingement-effusion cooling behavior in a curve effusion wall of combustion chamber. T- type thermocouples were used for measuring the temperature distribution of effusion wall. The test results showed that the discharge coefficient was increased with the increasing blowing ratio. Muwafag and Reyadh [7] used infrared camera to examine experimentally the effect of the holes density of adiabatic effusion test plate on the film cooling

effectiveness. They found that the film cooling effectiveness increase with increasing holes density. Assim and Humam [8] investigated experimentally the film cooling effectiveness of two staggered rows holes with arc trench. Infrared camera was used to measure the surface temperature. At low blowing ratio, the arc trench gives high film cooling effectiveness than the rectangular trench.

Few studies have been conducted to estimate the performance of impingement/effusion cooling system. Most of these studies for the three - cooling system were concentrated on the adiabatic test surface, while few studies were done with small scoop on a metal test surface (i.e., adiabatic and conduction heat transfer). As a matter of fact at present study, the wall cooling effectiveness (η) is regarded as suitable criteria to compare the impingement with impingement/effusion cooling systems.

However, the present work aims at experimentally analyzing the heat transfer characteristics of using multiple impingement jets and impingement/effusion on a metal test surface (i.e., adiabatic and conduction heat transfer with the variation of the most effective parameters that governed both systems. In present test, for impingement case, the exit flow is after impingement on the target to ambient while for impingement/effusion case, the exit flow is through effusion holes.

Experimental Set-up and Procedures

The test rig consists of two open loops, mainstream and secondary flows loops, as shown in figure (1). The impingement jets from plenum are heated, and the coolant is the main flow. The mainstream loop includes air blower, settling chamber, grid screen, and Pitot-static. The secondary flow loop contains turbo blower, orifice meter, heaters, by-pass line, plenum chamber that contains stainless steel mesh to create uniform flow, and pressure tapping. Both loops have temperature sensors to measure the temperature of the mainstream and secondary flows. The philosophy in both cooling and heating wall effectiveness evaluation concept is the same; the wall target is heated instead of cooling to save energy. The mainstream flow condition was fixed at (V_∞ = 20 m/s) and (T_∞= 40^0C), and the secondary flow condition was (T_s=100^0C) with varied mass flow rate according to the desired Reynolds number. Most impinging jet industrial applications involve turbulent flow ($Re_j > 1000$) in the whole domain downstream of the nozzle. Thus, the flow was regarded as turbulent, and$Re_j$was taken as 5000, 75000, 10000, 12000, and 15000 with equivalent effusion (BR = 1, 1.4, 1.9, 2.24, and 2.8). Thermocouples type K were used to measure the mainstream flow temperature and secondary flow temperature, such as jet inlet, jet exit, and the secondary flow exit (cross flow exit).

The investigation was performed in an open rectangular duct that has dimensions (5 cm) width, (13 cm) height, and (23 cm) length. The impingement experimental set-up contains the secondary flow that passes through the plenum duct and impacts the inner surface of the test plate, while the mainstream flow works as a resistive film on the outer surface of the target plate, then both flows leave the test section separately, as depicted in figure (2-a). For impingement/effusion case, the secondary flow impacts the target surface and then effuses with the mainstream flow and the mixed stream exhausts from

the exit duct, as seen in Figure (2-b). The back side of the plenum is insulated to insure that there is no heat transfer from or to the test section.

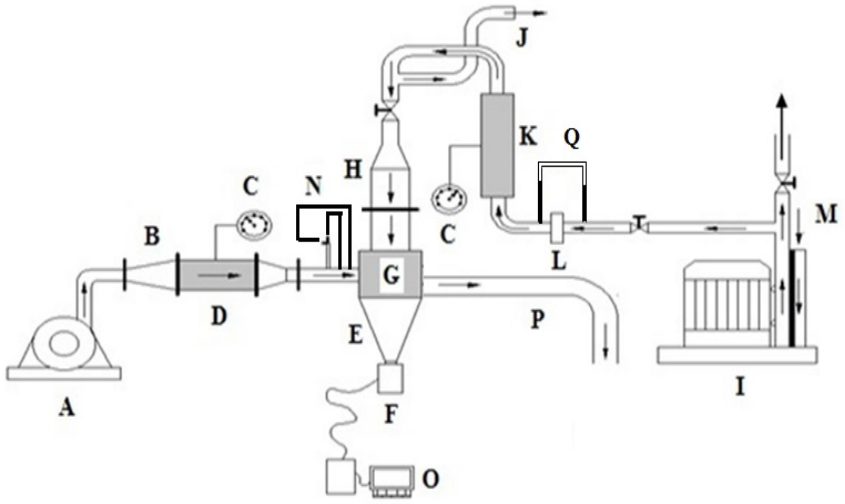

A. Air blower (Mainstream flow)
B. Diffuser
C. Variac
D. Settling chamber
E. Camera window
F. Infrared camera
G. Test section
H. Plenum
Q. Manometer

I. Air blower (Secondary flow)
J. Transition line
K. Air heater
L. Orifice meter
M. Suction side
N. Pitot tube with manometer
O. PC computer
P. Exhaust duct

Figure (1): Experimental test rig set-up

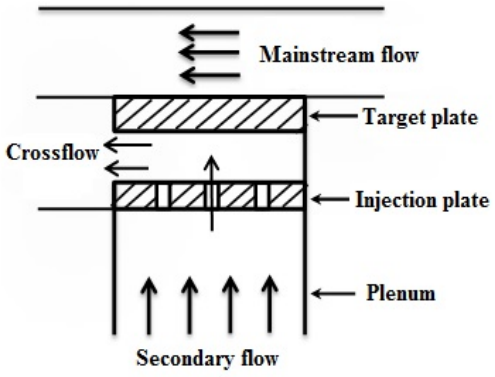

(a) Impingement case test section

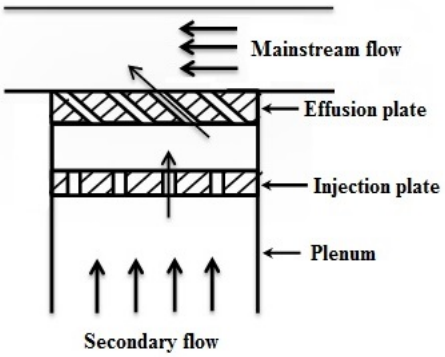

(b) Impingement/Effusion case test section

Figure (2): Schematic of Test section

The measured thermodynamics properties in present investigation are the plenum chamber entry temperature (T_{in}), the jet temperature (T_j), mainstream temperature (T_∞), the target outer surface temperature(Tw_O) and mass flow rate of the secondary flow ($\dot{m}$). The infrared thermograph (IR) system was used to measure the target outer surface temperature (Tw_O). (IR) system is greatly affected by both background temperature and local emissivity. The target outer surface was sprayed with mat black color and regarded as a perfect black body to increase the emissivity.

Numerical work

A numerical study is introduced to physically explain the flow characteristics and the phenomena associated with flow field in the jet impingement area. ANSYS FLUENT 14 package is used to perform the numerical simulation of the jet impingement system. Three–dimensional model is introduced, second order upwind is selected for discreteness of the governing equations, and standard (k–ϵ) turbulence model is applied.

A SOLID WORK PREMIUM 2012 was used to draw the geometry of the experimental model. The height of mainstream and secondary flows passages (in y-direction) are chosen as 50 mm and 30 mm, respectively. The width of the domain (in z-direction) is 50 mm and the length of the domain (in x- direction) is 200 mm. Unstructured mesh was used to discretize the computational domain into a finite number of control volumes by using the finite–volume scheme. Structured mesh is ruled out because it is favorable for easy cases and it becomes insufficient and time consumed for complicated geometries **[**9**]**. The model was meshed by GAMBIT software.

Assumptions

The following assumptions are used for air during the present study: steady state, Newtonian fluid, incompressible fluid, three dimensional and turbulent flow.

Grid Independency

Grid refinement tests for average static temperature on outer surface test plate indicated that a grad size of approximately (5 million cell) provide sufficient accuracy and resolution to be adopted as the standard for film cooling system. Figure (3) shows such example for the grid independency test performed for cooling system.

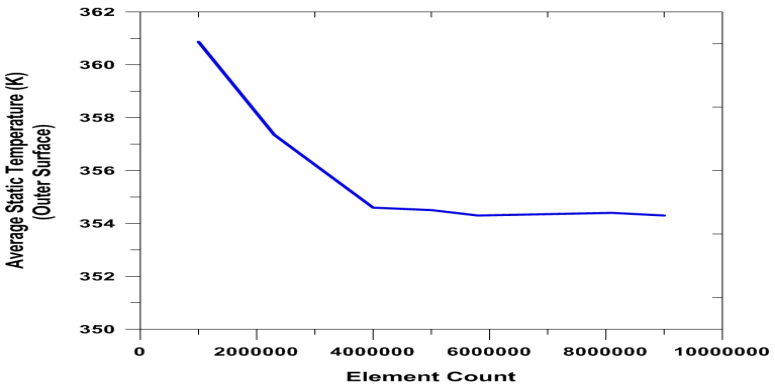

Figure (3): Grid independency test

Boundary Conditions

The impingement, target and effusion plates are regarded as solid boundary surfaces. The space of the secondary and mainstream flows is as the regarded fluid boundary condition. The boundary conditions of inlets of the mainstream and secondary flows are defined as velocity-inlet. The inlet temperatures for both secondary and mainstream flows are 100 ^{O}C and 40 ^{O}C, respectively, while the inlet velocity of mainstream flow is fixed at 20 m/s and secondary flow velocity is adjusted depending on the jet Reynolds number (Re_j) required values. Turbulent intensity (TU) for both flows is chosen according to Re_j and mainstream velocity values. The hydraulic diameter for both flows depends on the inlet flow geometry. The outlet domain is specified as pressure outlet which is depends on the experiment data for both flows. To reduce the amount of grids and calculation time, symmetric boundary condition is applied on one side of the geometry. The domain boundary conditions are given in the figures (4) and (5).

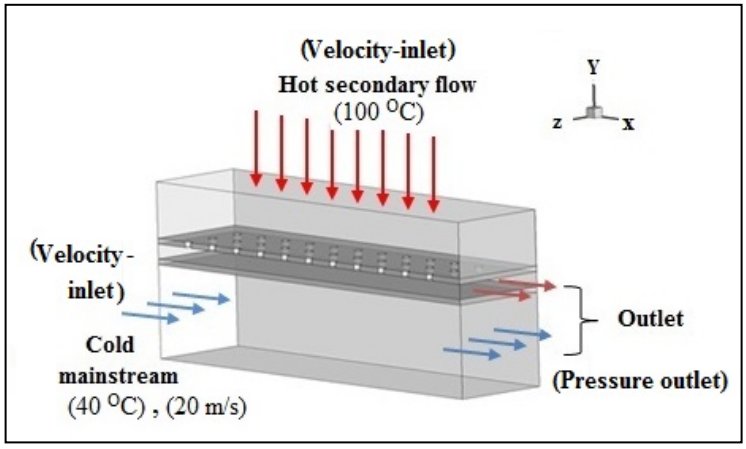

Figure (4): Schematic structure of impingement cooling case

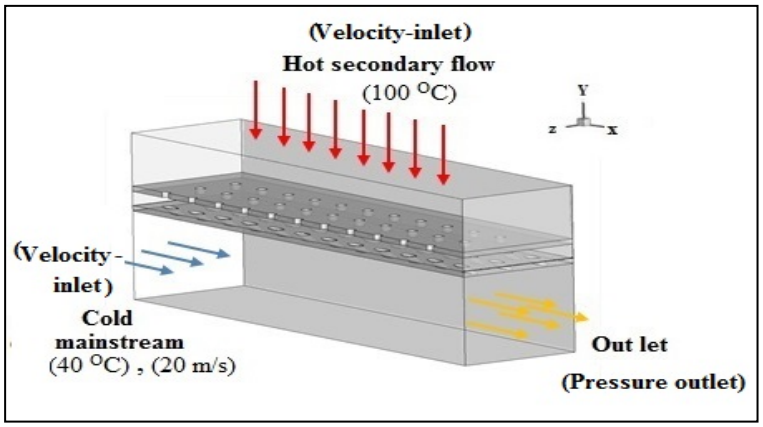

Figure(5): Schematic structure of impingement/effusion cooling case

Jet and Effusion Holes Geometry

The structural form of the impingement case contains two plates: injection plate and target plate, while for impingement/effusion case, the target plate works as a target and at same time effuses the secondary flow. The injection plate is made from aluminum, while target and target/effusion plates are made from stainless steel 304. The injection plate is perforated, and the holes are distributed in line array, as shown in figure (6). The target plate of impingement/effusion case is also perforated to work an effusion plate with inline holes arrangement. Jet and effusion holes are arranged in staggered manor, as illustrated in figure (7). For both cases, the test plates length and width are (200 mm) and (100 mm), respectively. The jet and effusion holes dimensions and geometries are listed in the table (1).

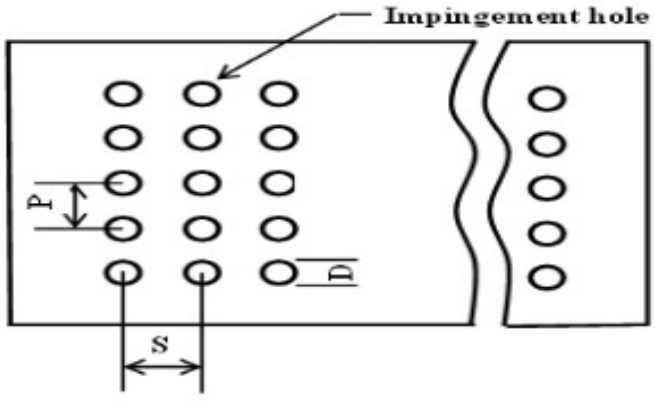

Figure (6) Impingement holes arrangement

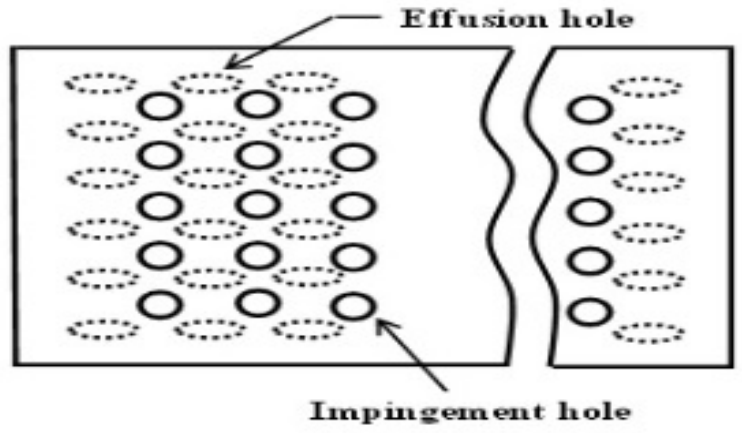

Figure(7): Impingement/effusion holes

Table (1) Jet and effusion holes dimensions geometries

Geometry	Impingement case		Impingement/Effusion case	
	Injection plate	Target plate	Injection plate	Effusion plate
D (mm)	4	-	4	4
Angles of injection& effusion	90^0	-	90^0	30^0
S/D	4	-	4	4
P/D	4	-	4	4
H/D	1.5 , 2 , 3		1.5 , 2 , 3	
No.of the holes	55	-	55	72
Re_j	5000 , 7500, 10000, 12500 15000	-	5000 , 7500, 10000, 12500 15000	-
BR	-	-	-	1, 1.4, 1.9, 2.24, 2.8
L/D	1	-	1	1.75
t (mm)	4	3.5	4	3.5
A (m^2)	0.02	0.02	0.02	0.02

Cooling effectiveness (η)

Cooling effectiveness is the most relevant parameter for measuring the performance of cooling system. Clearly, if the cooling effectiveness is non-existent, or zero, there is no cooling effect; whereas, if the cooling effectiveness is equal to unity, the liner metal and coolant temperature are the same. These two extreme values of either zero or unity are

considered as outer limits for the cooling effectiveness parameter. In general, the cooling effectiveness lies in-between these two limits and characterizes the performance of the cooling system [10]. Cooling effectiveness becomes a major criterion when different cooling techniques are considered. The non-dimensional wall cooling effectiveness is defined as:

$$\eta = \frac{T_\infty - Tw_o}{T_\infty - T_S} \quad \ldots (1)$$

The accuracy of the present experimental investigation is deduced from the methodology given in [11]. The uncertainty of cooling effectiveness is set up as $\pm$ 2.56 % .

6. Discharge Coefficient Evaluation (C_D)

The flow velocity and the geometrical parameters on the discharge coefficient can be calculated according to [12], the pressure losses at the impingement side are defined by the non-dimensional discharge coefficient as:

$$\Delta P = \frac{{m_i}_h{}^2}{2\,A_h{}^2 CD^2\,\rho}$$

Therefore,

$$C_D = \frac{m_{i_h}}{A_h\sqrt{2\,\rho\,\Delta P}} \quad \ldots (3)$$

The term (ΔP) represents the difference in the pressure across the impingement wall.

Comparisons between Numerical and Experimental Results

The wall cooling effectiveness (η) is used as the main criteria to compare the numerical and the experimental results for all cooling system. The comparisons are included samples results of two cooling systems (impingement and impingement/effusion). Figures (8) and (9) show the spanwise of average cooling effectiveness ($\eta_{sa.}$) for both results. Experimental results are lower than that of the computational results of (12.2%) and (8%) for impingement and impingement/effusion cases, respectively. The difference in results between the experimental and numerical values back to the heat losses and to the accuracy of measuring devices.

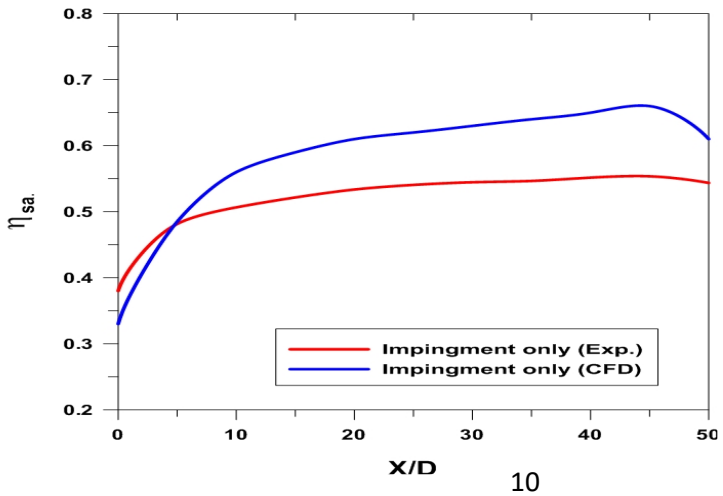

Figure (8): ($\eta_{sa.}$) verses (X/D) at (H/D=2) and (Re_j=5000)

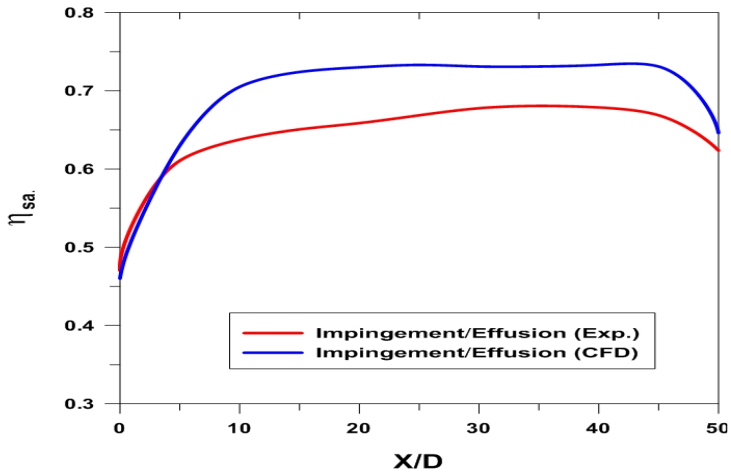

Figure (9): ($\eta_{sa.}$) verses (X/D) at (H/D=2) and (Re_j=5000)

Numerical results (Flow Feature)

The correct prediction of heat transfer rate needs a profound analysis and understanding of the flow field mechanism. As stated in the literature for impingement system, the optimum jet angle which gives high heat transfer is achieved at 90^0, where the maximum momentum of flow is strike on the target plate [13]. Also, it shows that the effects of hole length to diameter (L/D) was not significant for development of impingement jet when L/D is greater than unity [14]; therefore in present work, the study was constrained to L/D=1. The impingement/effusion cooling flow is characterized by sheer complexities. First, when the coolant ejected from the impinging holes cools the backside surface of effusion plate and second, the coolant which enters through and then discharges from the effusion holes, forms a coolant film near the surface of effusion plate subject to the mainstream flow[5]. The numerical study is accomplished to understand the flow patterns in impingement and impingement/effusion cooling systems, where the flow behavior is investigated through two plates. The optimum hole angle that found as mentioned before 90^0 and 30^0 was used for impingement and effusion holes, respectively. The flow characteristic of impinging jets for impingement and impingement/effusion cases at (Re_j= 5000) and ($H/D = 2$) in x-y plane is shown in the figure (10). For impingement case, the result shows the velocity vector within the cooling passage colored by temperature. The impingement jets are deflected away towards the downstream direction due to the effect of cross flow induced by upstream jets. The deflection becomes significant as the flow progresses downstream of the first raw. The momentum of the impingement jets is reduced due to the interaction with cross flow, and this affects the rate of heat transfer at stagnation region. This cross flow shows a positive enhancement on heat transfer at the downstream region where high momentum and flow

velocity are creating due to jet flow accumulation, and this will enhance the cooling effectiveness downstream direction, as shown in figure (15).
In the impingement/effusion system for the same geometry, two locations in the (x-y) plane were chosen to show the flows through the impingement holes (Z/D = 4) and effusion holes (Z/D = 6). It can be seen from the figure, the jet stagnation region behavior in the downstream direction is approximately unaffected due to the penetration of cross flow through the effusion holes. This leads to increase the wall cooling effectiveness as compared with the impingement system.

Experimental results

Wall Cooling Effectiveness

The variation of the average wall effectiveness ($\bar{\eta}$) with (Re_j) at different jet height ratios (H/D=1.5, 2, 3) are presented in figure (11) for impingement case. As seen, the wall effectiveness is increased as the Reynolds number increased for all values of H/D. Low values of ($\bar{\eta}$) are observed at ($H/D = 1.5$) with respect to that of ($H/D = 3$). The wall effectiveness is increased by (7.4 %) as (H/D) increased from 1.5 to 3. The narrow spacing between the two plates (jet and target plates) creates a highly constrained cross flow with high momentum and adds more back pressure. The presence of a strong momentum at low H/D tends to disturb the impinging jet pattern at the stagnation region and increases the boundary layer growth on the surface degrading the heat transfer rates, lowering the wall cooling effectiveness.

Generally, best performance is observed at ($H/D = 3$), since the optimum cross flow acceleration is maintained reducing the bad effect at the stagnation region, therefore high recirculation flow between the jets is achieved. These results are in good agreements with results of [15], where high heat transfer coefficient was recorded at H/D=3 with independent value of P/D for inline jet arrangement. Figure (12) shows for impingement/effusion case, the same type of results given in figure. (11). It is observed that at ($H/D = 2$), the best wall cooling effectiveness is obtained. The flow is passing through effusion holes that present a sufficient exit pathway, therefore lower cross flow effects are maintained than those of the impinging case, especially at ($H/D = 2$).

The average wall cooling effectiveness ($\bar{\eta}$) variation with (Re_j) is presented in Figures (13) and (14) at different (H/D) ratios. As seen from these figures, the impingement/effusion case enhanced the cooling effectiveness over that of the impingement case. The reason is back to the high additional heat transfer afforded by effusion film cooling. The maximum increment in ($\bar{\eta}$) for impingement/effusion case is observed at ($H/D = 2$), of about 23% at (Re_j= 5000), 16 % for (Re_j= 7500), and 14% at (Re_j= 15000).

Figure (15) shows the contour of local cooling effectiveness at the outer surface of test plate for impingement and impingement/effusion cases under the variation of (Re_j) at ($H/D = 2$). This contour was obtained by using the images of infrared camera and applying the equation (1). For impingement case, the results depict that the wall cooling effectiveness (η) increases gradually in downstream direction, this was due to increase in flow velocity between the jet plate and the target plate (cross flow) along the stream direction. This indicates that the cross flow have a dual effect on cooling performance; it

decreased the cooling effectiveness at impingements region while it increased the cooling performance at the region around the impingement jets. The effective area of the impingement jets is approximately 40% of the total heat transfer area of the tested plate of X/D=4, therefore the cross flow shows domination in heat transfer enhancement over the impingements jets, especially at downstream where the cross flow velocity are high.
For impingement/effusion case, it can be seen clearly that the distribution of (η) is uniform, especially at high (Re_j) values. The reason for this back to the dissipation of the cross flow through the effusion holes in the mainstream flow and to the arrangement of the impingement holes that was aligned in the mid region where the effusion holes around the impingement stagnation point.

The average spanwise cooling effectiveness ($\eta_{sa.}$) along the downstream flow direction (X) for both cases is shown in the Figures (16 to 19). ($\eta_{sa.}$) was calculated from the temperature distribution on the outer surface target plate. For impingement case, the cooling effectiveness is increased along the flow direction up to downstream distance of X/D=30. Optimum cooling is achieved at X/D= 40, and slight drop is observed in the region of X/D>40, this contributed to the effect of cross flow as stated above. As seen ($\eta_{sa.}$) for impingement/effusion case, the blowing ratio greatly affects the cooling behavior. At the effusion wall, ($\eta_{sa.}$) increased slowly and kept a steady value in subsequence at BR>2. ($\eta_{sa.}$) values are increased with increasing (Re_j) at all mainstream positions except at (Re_j = 12000 equivalent BR =2.24 and 15000 equivalent BR =2.8) and the reason backs to BR values (BR>2). Meanwhile, the effusion blowing ratio takes an evident effect on ($\eta_{sa.}$).

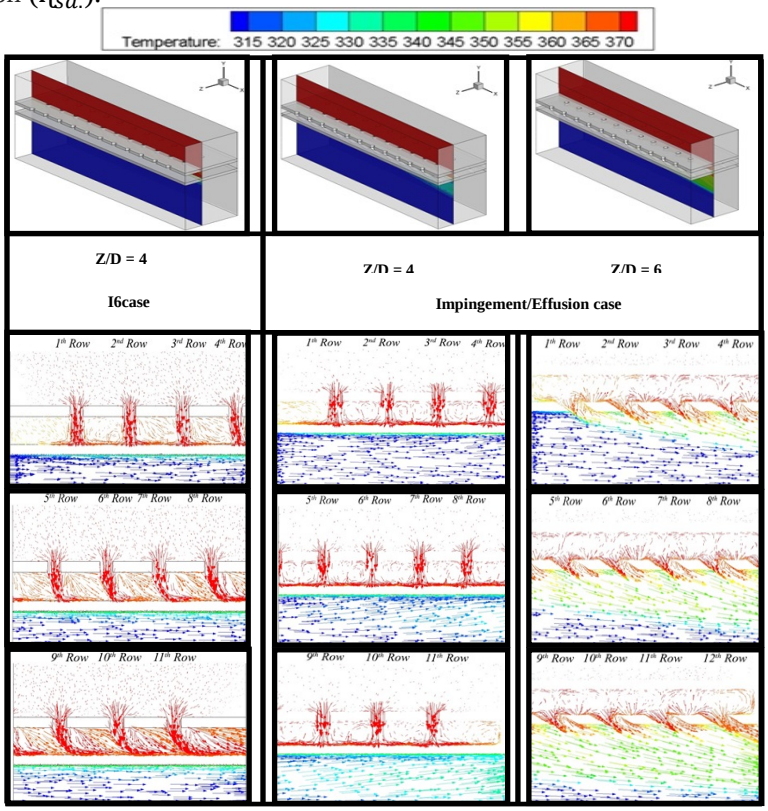

Figure (10): Flow vectors colored by temperature in (x-y) plane at$(H/D = 2)$ and (Re_j= 5000)

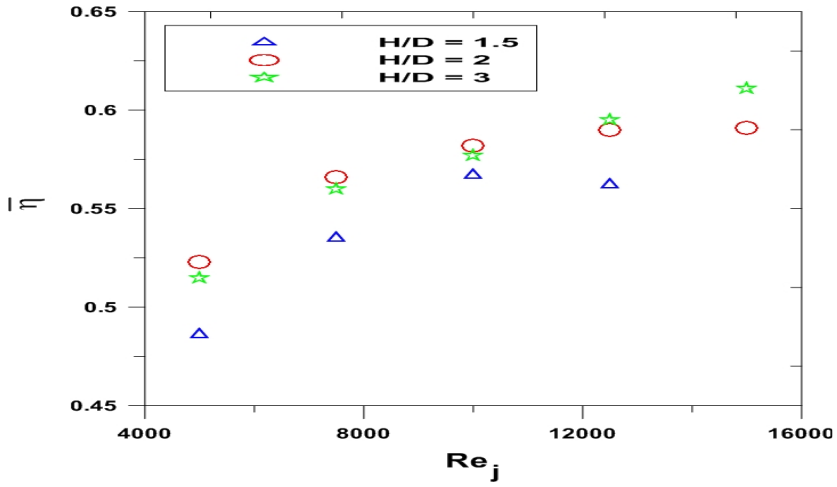

Figure (11): Effect of (H/D) & (Re_j) on $(\bar{\eta})$ (Impingement case)

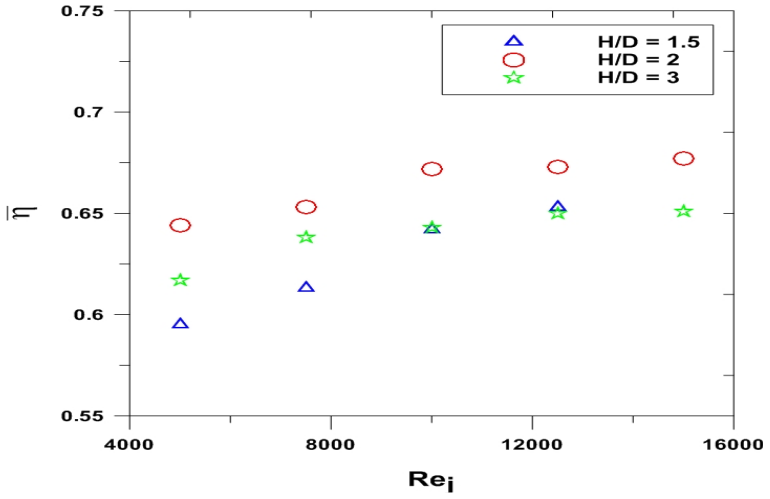

Figure (12): Effect of (H/D) & (Re_j)on $(\bar{\eta})$ (Impingement/Effusion case)

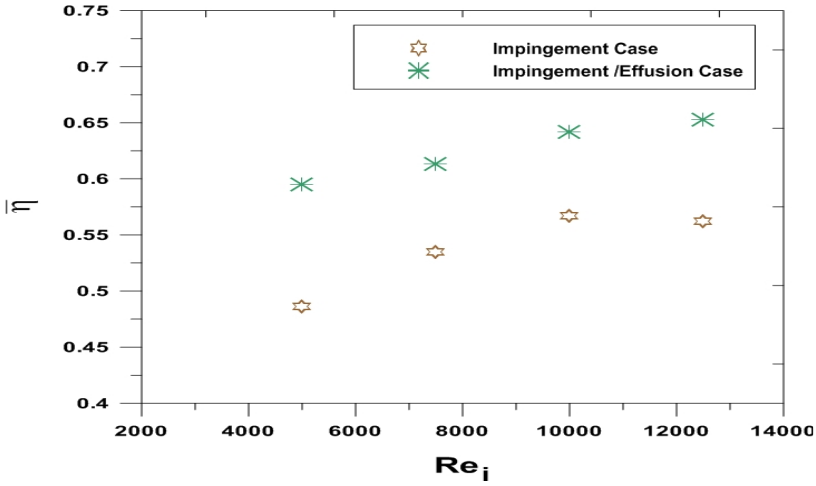

Figure (13): ($\bar{\eta}$) verses (Re_j) for (H/D=1.5)

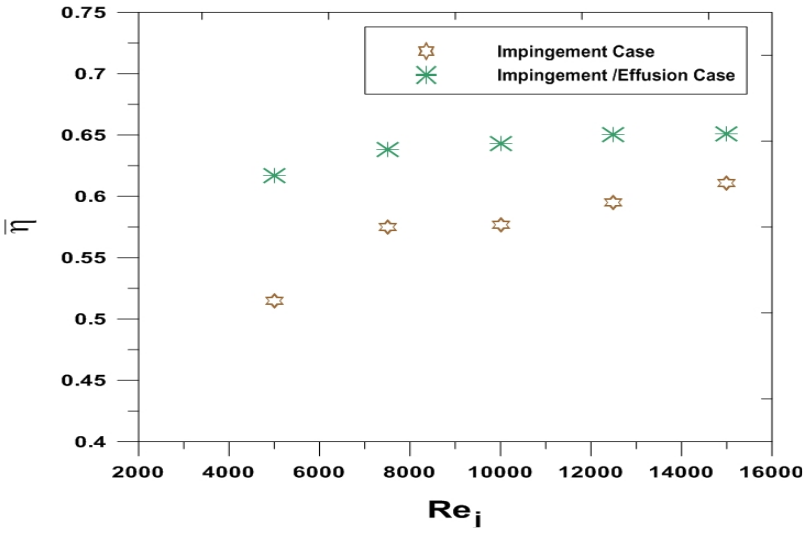

Figure (14): ($\bar{\eta}$) verses (Re_j) for (H/D=3)

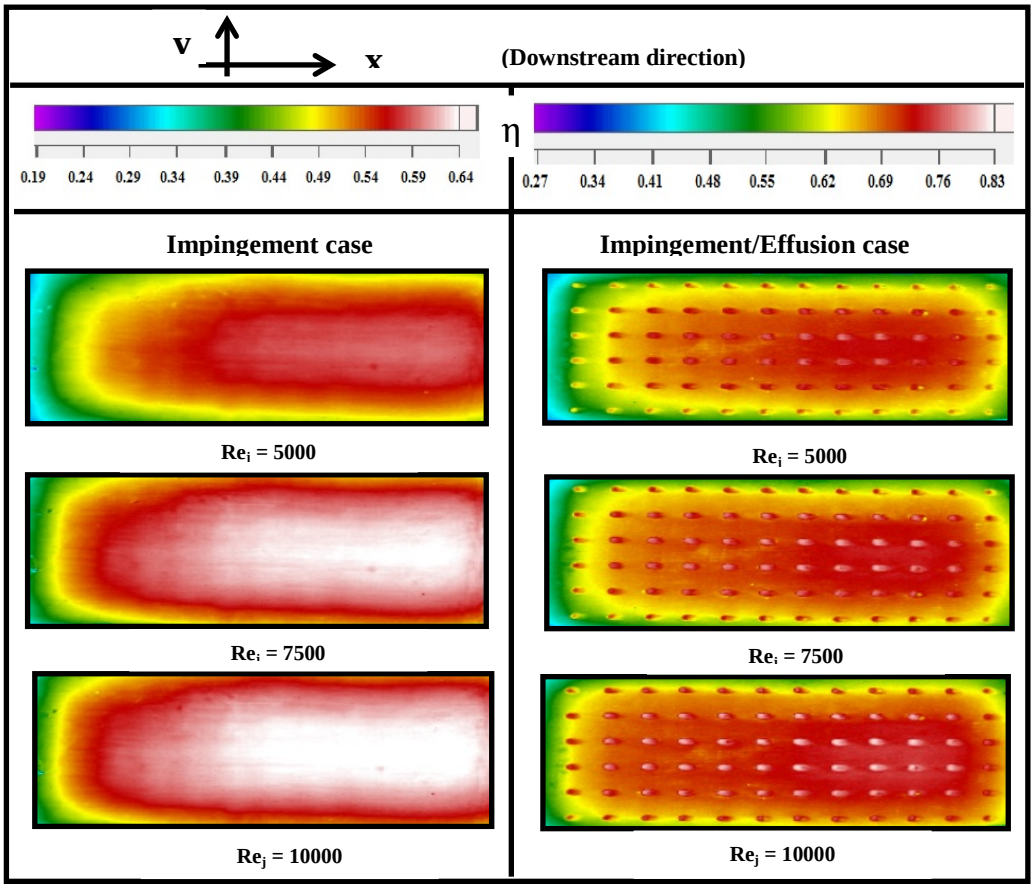

Figure (15): Cooling effectiveness contour of the outer surface target plate at (H/D=2). (Exp.)

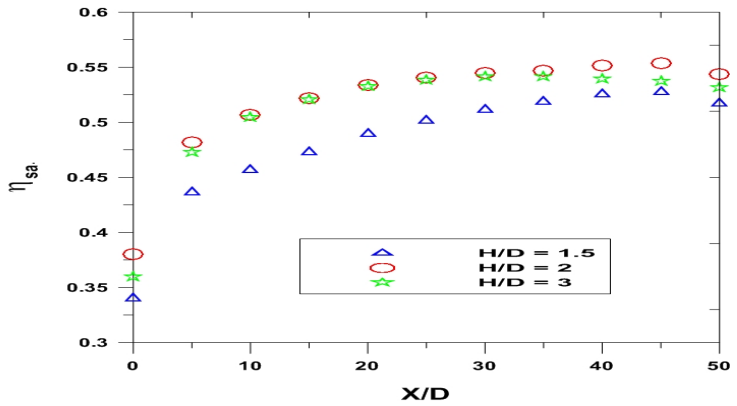

Figure (16): Distribution of ($\eta_{sa.}$) at (Re = 5000) (Impingement case)

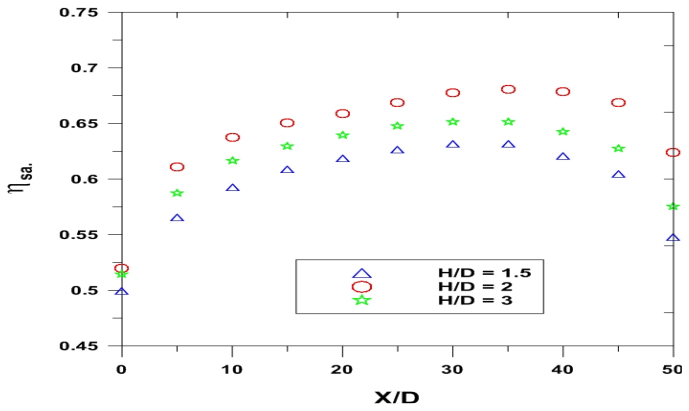

Figure (17): Distribution of ($\eta_{sa.}$) at (Re=5000) (Impingement / Effusion case)

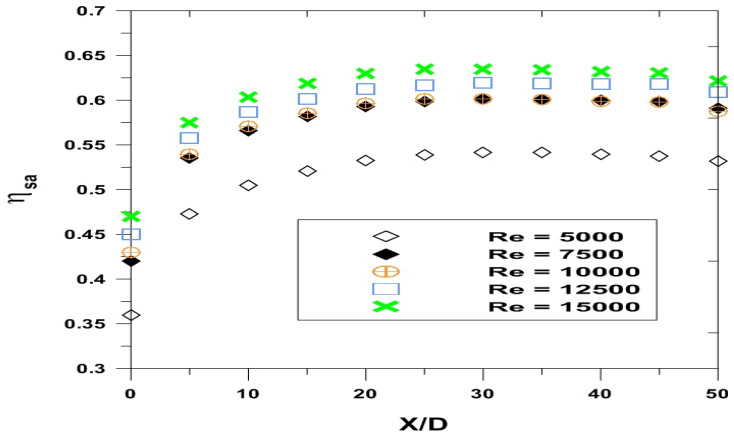

Figure (18): Distribution of ($\eta_{sa.}$) at (H/D = 3) (Impingement case)

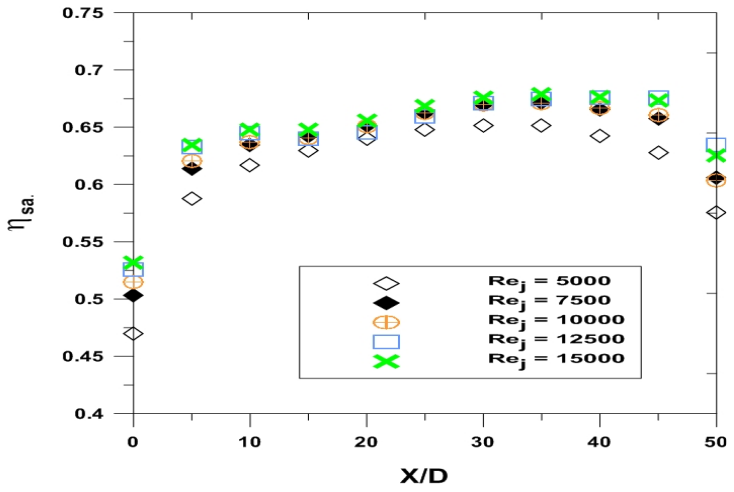

Figure (19): Distribution of ($\eta_{sa.}$) at (H/D = 3) (Impingement /Effusion case)

Pressure Losses and Discharge Coefficient

The pressure losses at the impingement side are related to the discharge coefficient (C_D). Figures (20) and (21) depict the influence of (H/D) on the discharge coefficient (C_D) for both impingement and impingement/effusion cases. For both cases, (C_D) is increased slightly with a constant level from ($Re_j = .5000$, BR=1 to $Re_j = 10000$, BR = 1.9). The present test results agree well with the results given by [6] of impingement/effusion cooling and [16] for impingement cooling case of combustion chamber. Both results showed that the discharge coefficient increased slightly with increasing BR. At ($Re_j > 10000$), the results disagreed with [6], since (C_D) kept at constant values, while at ($Re_j \geq 12000$), the (C_D) values decreased slightly. For impingement case at ($H/D = 1.5$), low (C_D) values were observed in which at($H/D = 1.5$), the strong cross flow adds additional back pressure to recover the pressure lost at the impinging side, while (C_D) conducted higher values at ($H/D = 3$). The main points raised here are for impingement case (Re_j) that play an important role but is still not as influential as (H/D) for (C_D) values. For impingement/effusion case, the secondary flow has sufficient effused holes to exit, a very slight change was observed in (C_D) values at (H/D = 2 and 3) cases.

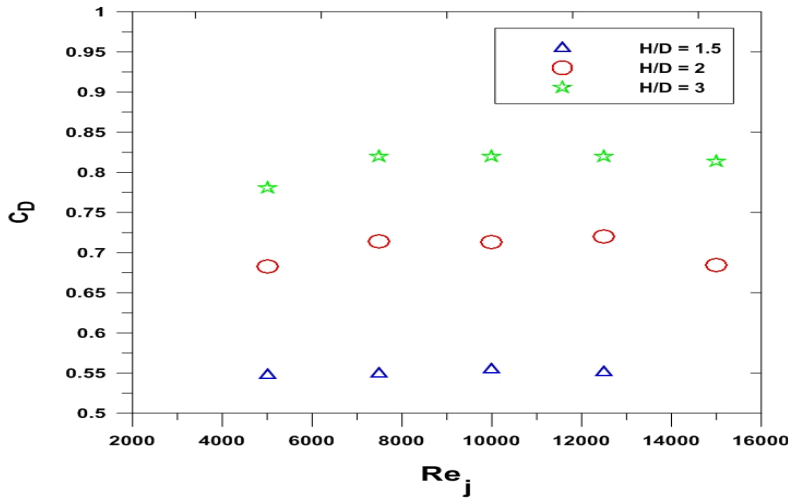

Figure(20): Influence of (H/D) and (Re_j) on (C_D) (Impingement case)

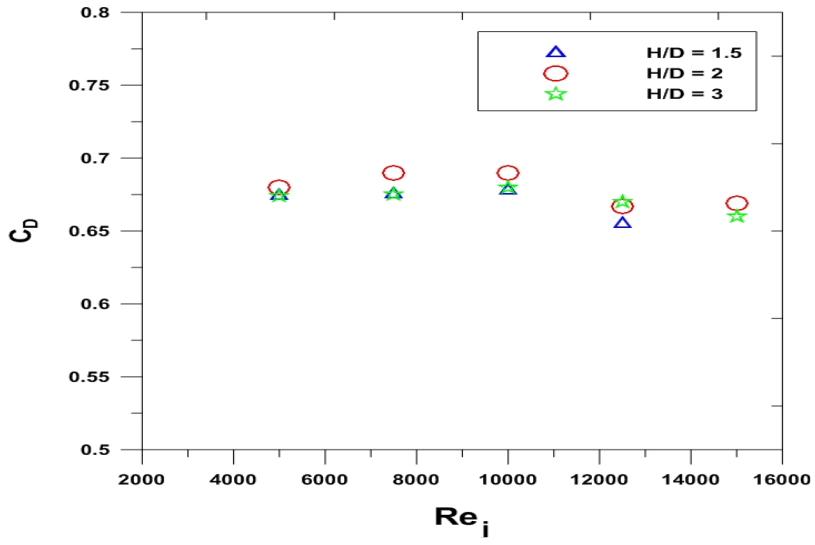

Figure (21){: Influence of (H/D) and (Re_j) on (C_D) (Impingement / Effusion case)

Conclusions

The performance analysis of impingement and impingement/effusion cooling systems investigated experimentally has reached the following conclusions:

1- Numerical prediction of the flow field structure for impingement case showed the effect of cross flow on the shift jet stagnation point. Thus, the cross flow has major effects on cooling performance while, the flow structure of impingement/effusion system showed decay the influence of cross flow on the stagnation point, therefore the impingement/effusion case gives better enhancement in (η) than impingement case.

2- The impingement/effusion case gives better enhancement in wall cooling effectiveness at ($H/D = 2$) of about 23% at (Re_j= 5000), 16 % for (Re_j= 7500) and 14% at (Re_j= 15000).

3- Both jets spacing in impingement case and blowing ratio in impingement/effusion case have an evident effect on the discharge coefficient. For impingement case, low (C_D) values were obtained at jet spacing 1.5 and high (C_D) at jet spacing 3.0. For impingement/effusion case, there was a very slight change in (C_D) values at jet spacing 2.0 and 3.0.

References

[1].AL Dabagh A. M., Andrews G. E., Abdul Husain R. A. A., Husain C. I., NazariA., and Wu J., (1990), "Impingement /effusion cooling : The influence of the number of impingement holes .and pressure loss on the heat transfer coefficient", ASME, Journal of Turbomachinary,Vol.112, pp. (467-476).

[2].Hyung H.C., and Dong H. R., (2001), "Local heat/mass transfer measurement on the effusion plate in impingement/effusion cooling system", ASME Journal of Turbomachinary, Vol. 123, pp. (601-608).

[3].Yong W.N., Dong H. R., and Hyung H. C.,(2003),"Heat transfer in impingement/effusion cooling system with rib turbulators", International Gas Turbine Congress, Tokyo, November 2-7, 2003.

[4].Sang H.O., Dong H.L., Kyung M.K., Moon Y.K., and Hyung H.C., (2008), " Enhanced cooling effectiveness in full coverage film cooling system with impingement jets", ASME Turbo Expo 2008 : Power for land, sea and air GT 2008, June 9-13,2008, Berlin, Germany .

[5].Zhang J., Xie H., and Yang C., (2009), "Numerical study of flow and heat transfer characteristics of impingement/ effusion cooling", Chines Journal of Aeronautics, 22, pp. 343-348.

[6].Yang W., Cao J., Shi R., Hao X., and Song S.,(2011), "Experimental investigation on impingement/effusion film cooling behaviors in curve section", Acta Astronautics 86 Journal, pp. 1782-1789.

[7].Muwafag Sh., and Reyadh Ch., (2014), "Effect of Holes Arrangement on Effusion Cooling Performance", Eng. & Tech. Journal, Vol. 32, Part (A), No. 4, University of technology, Iraq.

[8].Assim H. Y., and Humam K. J., (2014), "Film Cooling from Two Staggered Holes Rows of Opposite Injection Angles with Downstream Row Embedded in Arc Trench", Eng. & Tech. Journal, Vol. 32, Part (A), No. 1, University of technology, Iraq.
[9]. "Fluent 14 use‹ guide, programing and tutorial guide", Fluent, Version 14, Ansys Inc., 2010.
[10].Frank J. C., (2006), "Heat transfer analysis", The Gas Turbine Handbook, 4.4, pp. (389-410).
[11].Kline S. J., and Mcclintock F. A., (1953), "Describing uncertainties in single sample experimental", Mechanical Engineering, Vol. 75, pp. 3-8.
[12].Amer. M. H, "Compact heat exchanger design using enhanced effective heat transfer", Ph.D. thesis submitted to the Department of Fuel and Energy, University of Leeds, 1991.
[13].Lamyaa A. E., and Deborah A.K., (2005),"Experimental investigation of local heat transfer distribution on smooth and roughened surfaces under an array of angled impinging", ASME Journal of turbomachinery, Vol.127, pp. 590-597.
[14].Andrew G. E., Durance J., Hussain C. I. and Ojobor S. N., (1987), "Full coverage impingement heat transfer: influence of the number of holes", ASME, Journal of Turbomachinary, Vol.109, pp. (557-563).
[15].Brevet P. , Dejeu C. , Dorignac E. , Jolly M. , and Vullierme J. J., (2002) "Heat transfer to a row of impinging jets in consideration of optimization", International journal of heat and mass transfer 45, pp. 4191-4200.
[16].Facchini M., and Surace M., (2006), "Impingement cooling for modern combustors: experimental analysis of heat transfer and effectiveness", Published online: 13 January 2006, Springer-verlag,